CORE
Metadata, citation and similar papers at core.ac.uk
Provided by IntechOpen

We are IntechOpen, the world's leading publisher of Open Access books
Built by scientists, for scientists

4,800
Open access books available

122,000
International authors and editors

135M
Downloads

154
Countries delivered to

Our authors are among the
TOP 1%
most cited scientists

12.2%
Contributors from top 500 universities

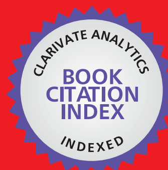

WEB OF SCIENCE™

Selection of our books indexed in the Book Citation Index in Web of Science™ Core Collection (BKCI)

Interested in publishing with us? Contact book.department@intechopen.com

Numbers displayed above are based on latest data collected.
For more information visit www.intechopen.com

Chapter 14

Materials Characterization Using Microwave Waveguide Systems

Kok Yeow You

Additional information is available at the end of the chapter

http://dx.doi.org/10.5772/66230

Abstract

This chapter reviews the application and characterization of material that uses the microwave waveguide systems. For macroscopic characterization, three properties of the material are often tested: complex permittivity, complex permeability and conductivity. Based on the experimental setup and sub-principle of measurements, microwave measurement techniques can be categorized into either resonant technique or nonresonant technique. In this chapter, calibration procedures for non-resonant technique are described. The aperture of open-ended coaxial waveguide has been calibrated using Open-Short-Load procedures. On the other hand, the apertures of rectangular waveguides have been calibrated by using Short-Offset-Offset Short procedures and Through-Reflect-Line calibration kits. Besides, the extraction process of complex permittivity and complex permeability of the material which use the waveguide systems is discussed. For one-port measurement, direct and inverse solutions have been utilized to derive complex permittivity and complex permeability from measured reflection coefficient. For two-port measurement, in general, the material filled in the waveguide has been conventional practice to measure the reflection coefficient and the transmission coefficient by using Nicholson-Ross-Weir (NRW) routines and convert these measurements to relative permittivity, ε_r and relative permeability, μ_r. In addition, this chapter also presents the calculation of dielectric properties based on the difference in the phase shifts for the measured transmission coefficients between the air and the material.

Keywords: microwave waveguides, relative permittivity, relative permeability, conductivity, resonant methods, nonresonant methods, materials characterization

1. Introduction

For macroscopic material characteristic investigations, three properties of the material are often measured: relative permittivity ε_r, relative permeability μ_r and conductivity σ. Normally, many microwave measurements only focus on the properties of relative permittivity, ε_r rather

INTECH
open science | open minds

© 2017 The Author(s). Licensee InTech. This chapter is distributed under the terms of the Creative Commons Attribution License (http://creativecommons.org/licenses/by/3.0), which permits unrestricted use, distribution, and reproduction in any medium, provided the original work is properly cited.

than the permeability μ_r and the conductivity σ. Recently, there has been an increased interest in the determination of dielectric properties of materials at microwave frequencies range. This is because those properties were played the important roles in the construction of high-frequency electronic components, the superconducting material properties, the quality of printed circuit board (PCB) substrate, the efficiency of microwave absorption materials, metamaterial characterizations and the performance of dielectric antenna design. Based on the setup and sub-principle of measurements, measurement techniques can be categorized into either resonant methods or nonresonant methods. In practice, the prime considerations in measuring the dielectric properties of the materials are the thickness required of the material, the size of the waveguide, limitations of the operating frequency and the accuracy of the measurements.

For material characterizing using resonant methods, a resonator is filled with a material or sample as shown in **Figure 1** [1, 2]. This produces a resonance frequency shift and also a broadening of the resonance curve compared to the resonator without filled with any sample. From measurements of shifting resonance frequency, the properties of the sample can then be characterized. The particular resonance frequency for the resonator without filled with the sample is depends on its shape and dimensions. The resonance measurement techniques are good choices for determining low-loss tangent, tanδ values for the low-loss sample, but such techniques cannot be used for the measurement of swept frequency.

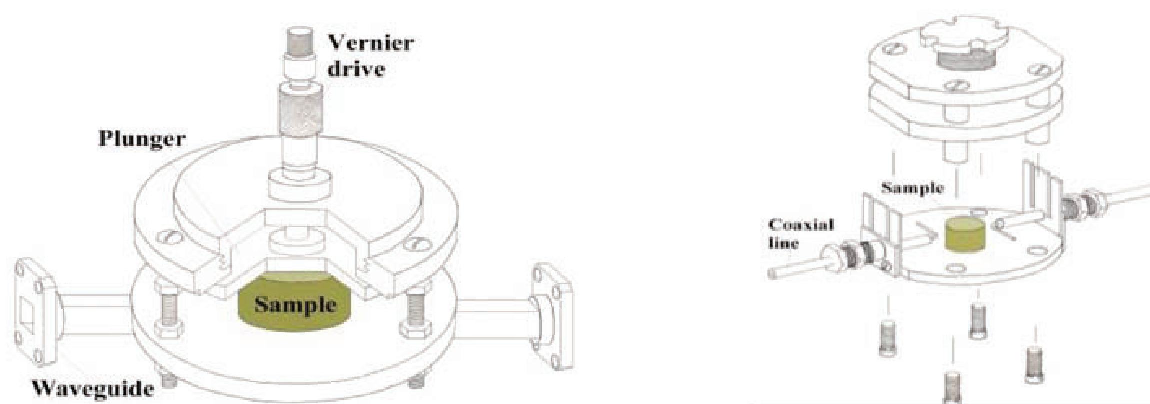

Figure 1. The resonator cavity filled with sample under test [1, 2].

A free-space and transmission/reflection measurement techniques are grouped in the category of nonresonant methods. The free-space technique is a far-field measurement, and a horn antenna is used as the radiator as shown in **Figure 2** [3–5]. The free-space method is suitable for the measurement for thin film sample with high temperature because horn radiators do not come into direct contact with the sample, and thus, the RF circuits of the instrument are safer from heat damage. However, this method provides a less precise measurement because the sensing field is highly dispersed. Furthermore, the distance between the sample surface and the horn aperture is difficult to gauge precisely. The coaxial, circular or rectangular waveguides are implemented in transmission/reflection measurement techniques which are directly

in contact with the sample. Although various measurement techniques are available to be used, when choosing the appropriate technique, some other factors are required to be considered in the selection of technique, such as accuracy, cost, samples shape and operating frequency. This chapter is focused only on coaxial and rectangular waveguides.

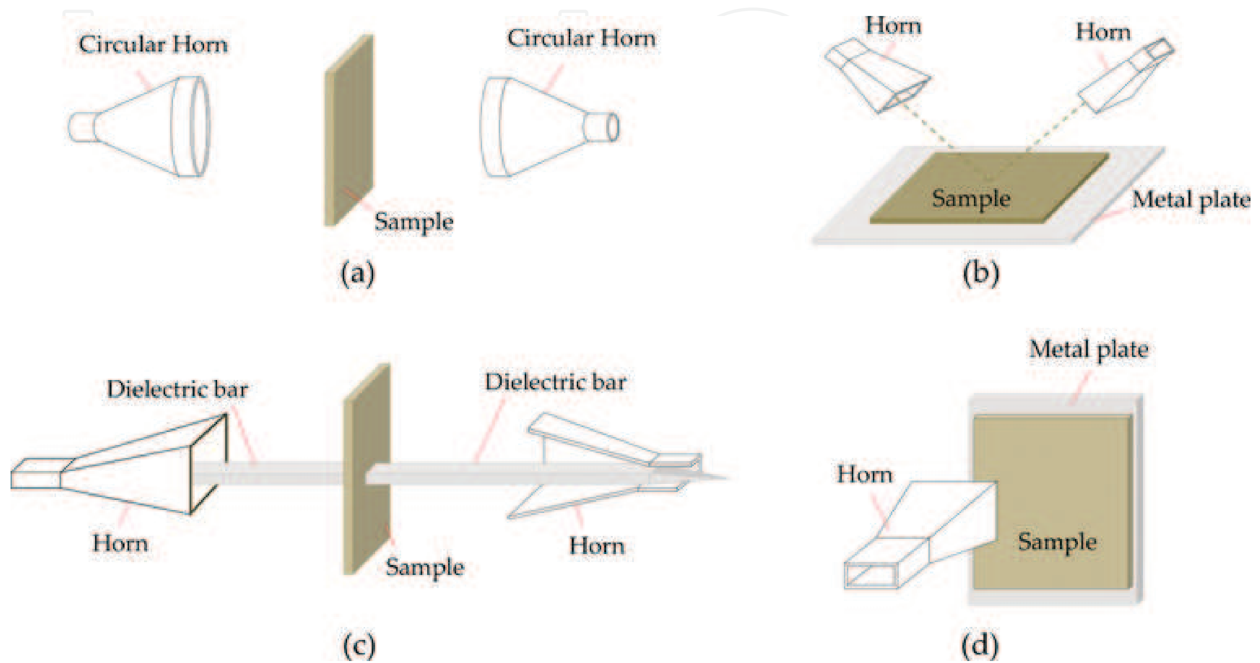

Figure 2. Free-space measurement setup for dielectric measurement of the thin sample [3–5].

2. Microwave measurement using coaxial and rectangular waveguides

2.1. Coaxial and rectangular waveguides

There are various sizes of the coaxial probes and rectangular waveguides, which are dependent on the operating frequency and its application. The coaxial probe is a waveguide consisting of inner and outer conductors, with radii a and b, respectively, as shown in **Figure 3**. On the other hand, the rectangular waveguide is a rectangular metal pipe with width, b and height, a, which guides high-frequency electromagnetic waves from one place to another without significant loss in intensity. There are several commercial rectangular waveguides, such as WR510, WR90, WR75 and WR62 waveguides, which covering a broad measurement range for L-band, X-band and Ku-band, respectively, as shown in **Figure 4**. Generally, the material characterization using waveguide discontinuity methods can be categorized into one-port and two-port measurements. The measurements assume that only the dominant transverse electric, TE_{10} mode propagates in the rectangular waveguide. On the other hand, only transverse electromagnetic mode (TEM) is assumed to be propagated in the coaxial line waveguide.

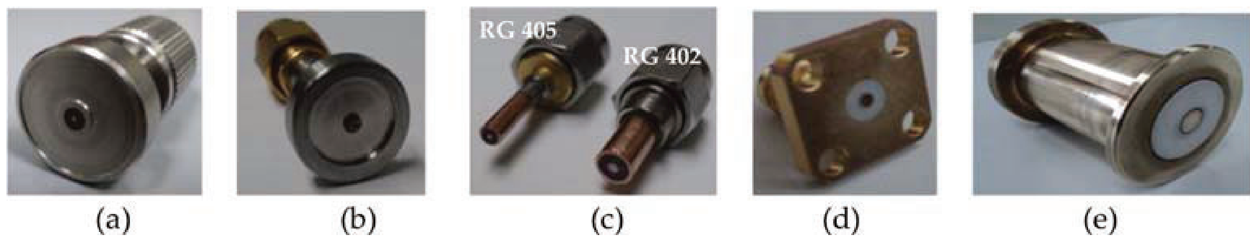

Figure 3. (a) Keysight dielectric probe kit with inner radius of outer conductor, b = 1.5 mm and radius of inner, a = 0.33 mm. (b) Customized small coaxial probe with b = 0.33 mm and a = 0.1 mm [6]. (c) RG402 and RG 405 semi-rigid coaxial probe [7]. (d) SMA stub coaxial probe with b = 2.05 mm and a = 0.65 mm [8]. (e) Customized large coaxial probe with b = 24 mm and a = 7.5 mm.

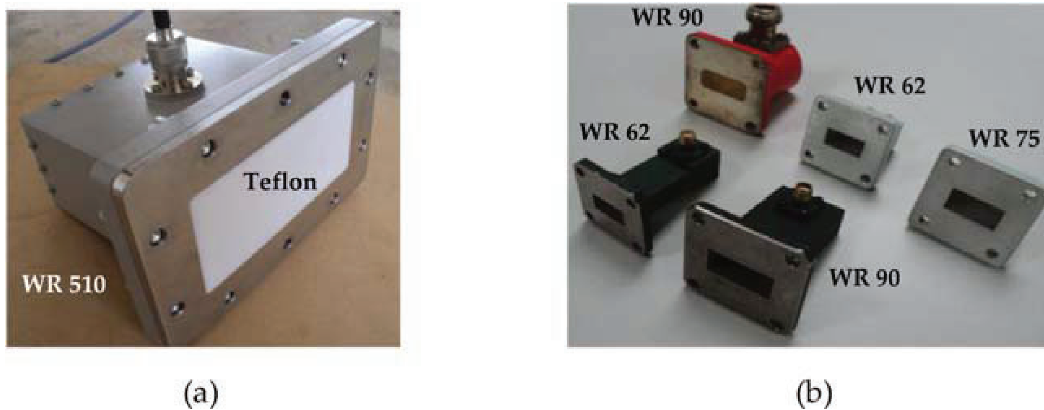

Figure 4. (a) WR510 waveguide-to-coaxial adapter and (b) WR 90, WR 75 and WR 62 waveguide-to-coaxial adapters [9].

2.2. Measurements principles

The one-port measurement is based on the principle that a reflected signal (reflection coefficient, S_{11}) through the waveguide, which end aperture is contacting firmly with the material under test (sample), will obtain the desired information about the material as shown in **Figure 5**. The main advantage of using one-port reflection technique is that the method is the simplest, broadband, nondestructive way to measure the dielectric properties of a material. However, one-port measurement is suitable only for measuring the relative permittivity, ε_r, of the dielectric material (nonmagnetic material, $\mu_r = 1$). This is due to insufficient information to predict the permeability, μ_r, if only obtained the measured reflection coefficient, S_{11} without transmission coefficient, S_{21}.

For **Figure 5a** and **c** measurements, the sample is considered infinite, as long as the sample thickness d is greater than the radius of the outer conductor b. However, the radiation, or sensing area, for an aperture rectangular waveguide is much greater than that of a coaxial probe. For instance, the WR90 waveguide has a radiation distance up to 20 cm in the air from the aperture waveguide. Hence, the sample under test must be much thicker when the rectangular waveguide is utilized in the measurement. Besides, the coaxial probe and rectangular waveguide are also capable of testing the thin film sample as shown in **Figure 5b** and **d**. The measurements required that the thin sample is backed by a metallic plate.

http://dx.doi.org/10.5772/66230

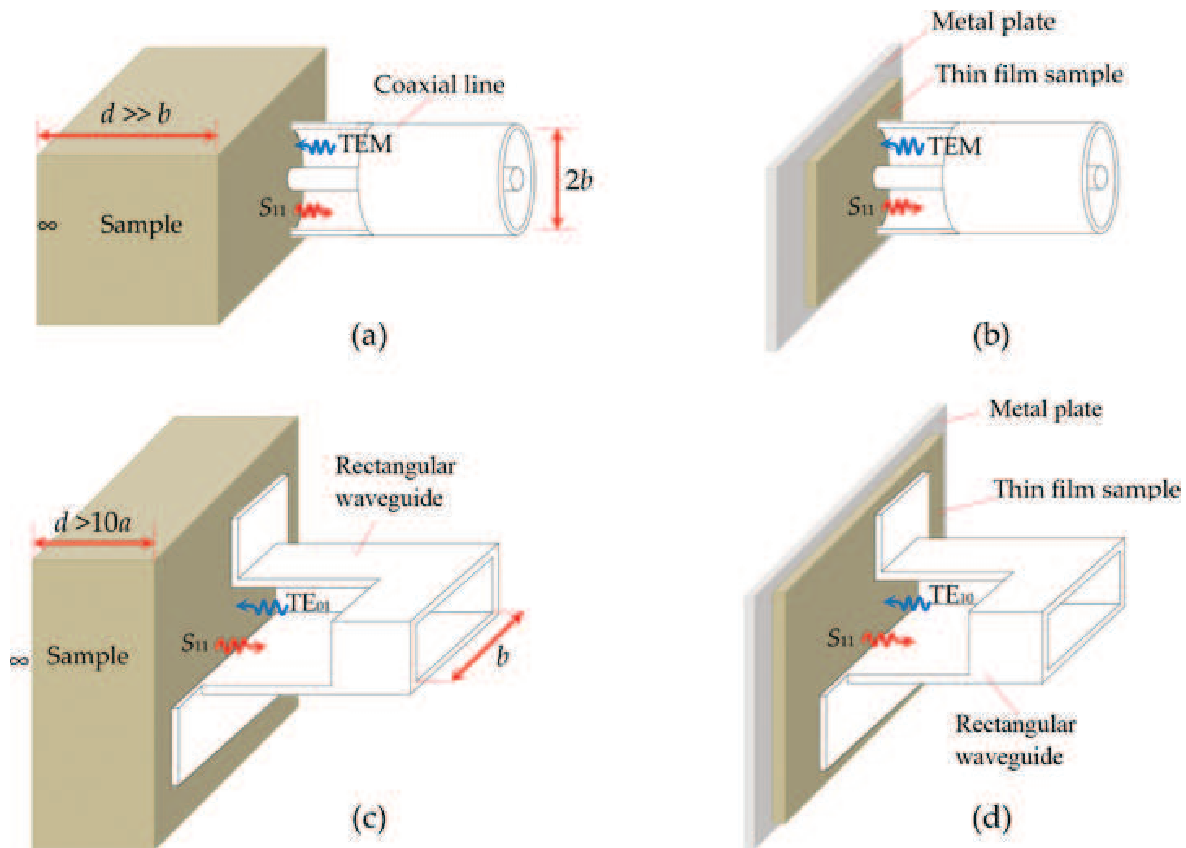

Figure 5. Open-port measurements using the (a), (b) coaxial probe and the (c), (d) rectangular waveguide.

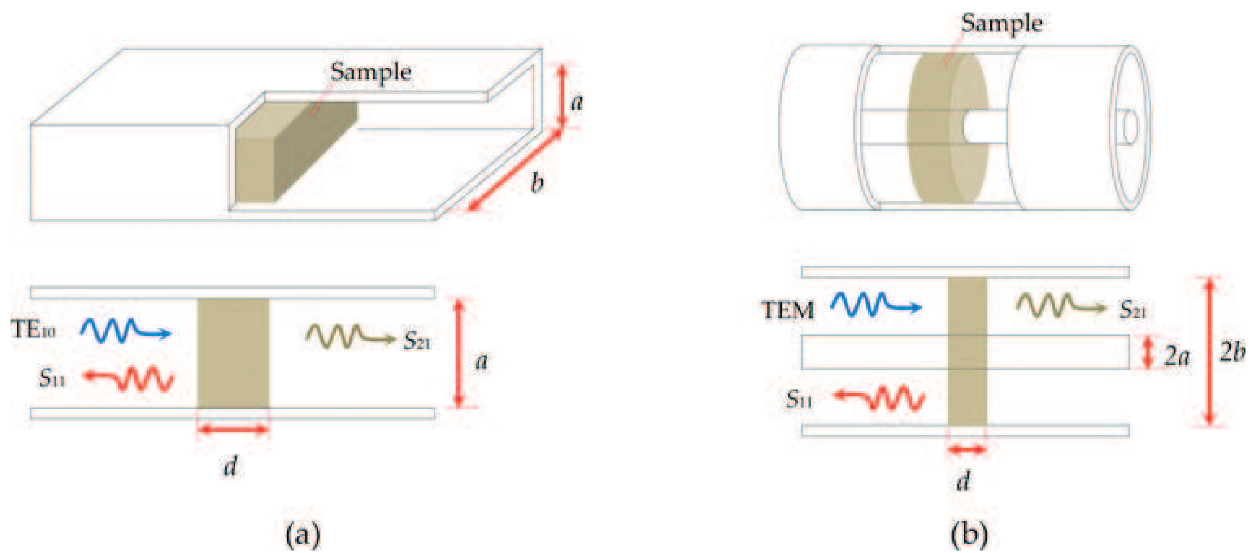

Figure 6. Two-port measurements using the (a) rectangular waveguide and the (b) coaxial transmission line.

The two-port measurement uses both reflection and transmission methods. Here, the material under test is placed between waveguide transmission lines or segments of the coaxial line as shown in **Figure 6**. The two-port measurement using coaxial or rectangular waveguides became popular due to the convenient formulations derived by Nicholson and Ross [10] in

1970, who introduced a broadband determination of the complex relative permittivity, ε_r and permeability, μ_r of materials from reflection and transmission coefficients (S_{11} and S_{21}). For measurements in **Figure 6**, the sample must be solid and carefully machined with parallel interfaces, and must perfectly fill in the whole cross section of the coaxial line or waveguide transmission line. The main advantage of using two-port Nicholson-Ross-Weir (NRW) technique [10, 11] is that the both relative permittivity, ε_r and relative permeability, μ_r of the sample can be predicted simultaneously. When using NRW method for thin samples, the thickness of the sample must be less than $\lambda/4$.

2.3. Measurements setup

In this chapter, the dimensions of the used coaxial probe and the rectangular waveguide as examples of the one-port measurement are shown in **Figure 7a** and **b**, respectively. The coaxial probe is capable of measuring the reflection coefficients covered the frequency range between 0.5 and 7 GHz. On the other hand, the rectangular waveguide adapter covers frequency from 8.2 to 12.4 GHz. For two-port measurement, a 5 cm length of the coaxial and the rectangular transmission lines is implemented. The experiment setup of the waveguides with an Agilent E5071C vector network analyzer (VNA) is shown in **Figure 8**.

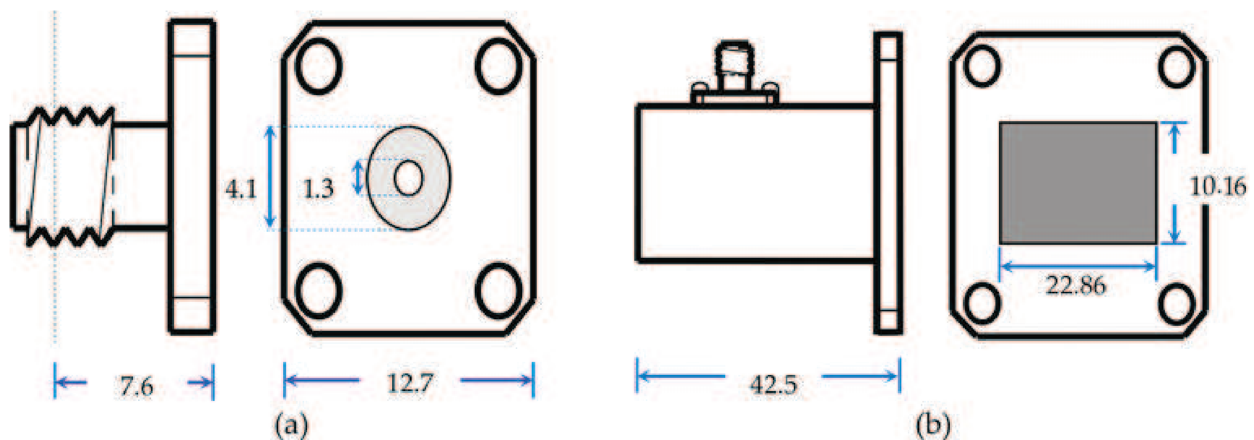

Figure 7. Cross-sectional and front views for the dimensions (in millimeter) of the (a) coaxial probe and the (b) rectangular waveguide.

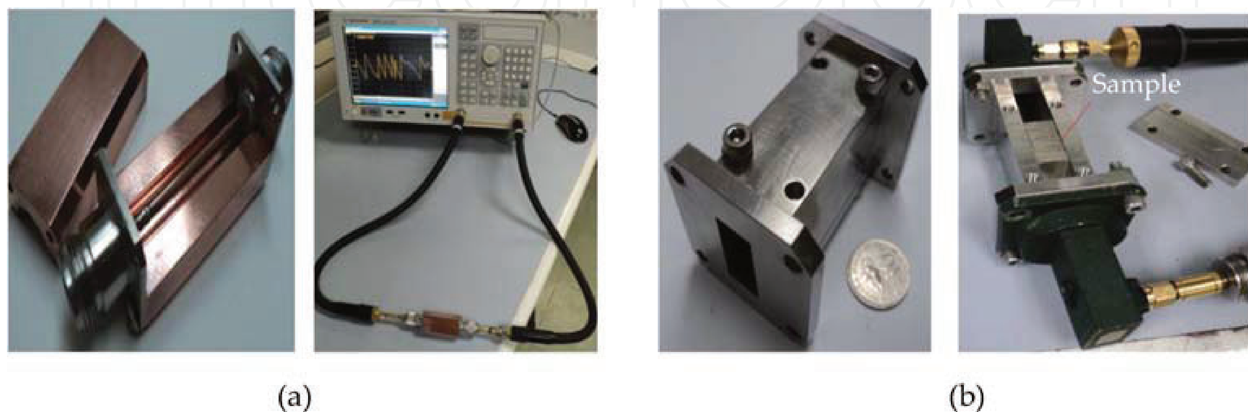

Figure 8. The experiment setup for the (a) coaxial cavity and the (b) rectangular waveguide cavity.

http://dx.doi.org/10.5772/66230

3. Waveguide calibrations

3.1. One-port calibrations

3.1.1. Open standard calibration

The reflection coefficient S_{11a_sample} of the sample at the probe aperture (at the BB' plane) should be measured as shown in **Figure 9b** [8]. However, during the measurement process, only the reflection coefficient S_{11m_sample} at the end of the coaxial line (at the AA' plane) is measured. The measured S_{11m_sample} must be calibrated due to the reflection at the AA' plane, which is separated from the sample (at the BB' plane) by a coaxial line. Thus, a de-embedding process should be done to remove the effects of the coaxial line.

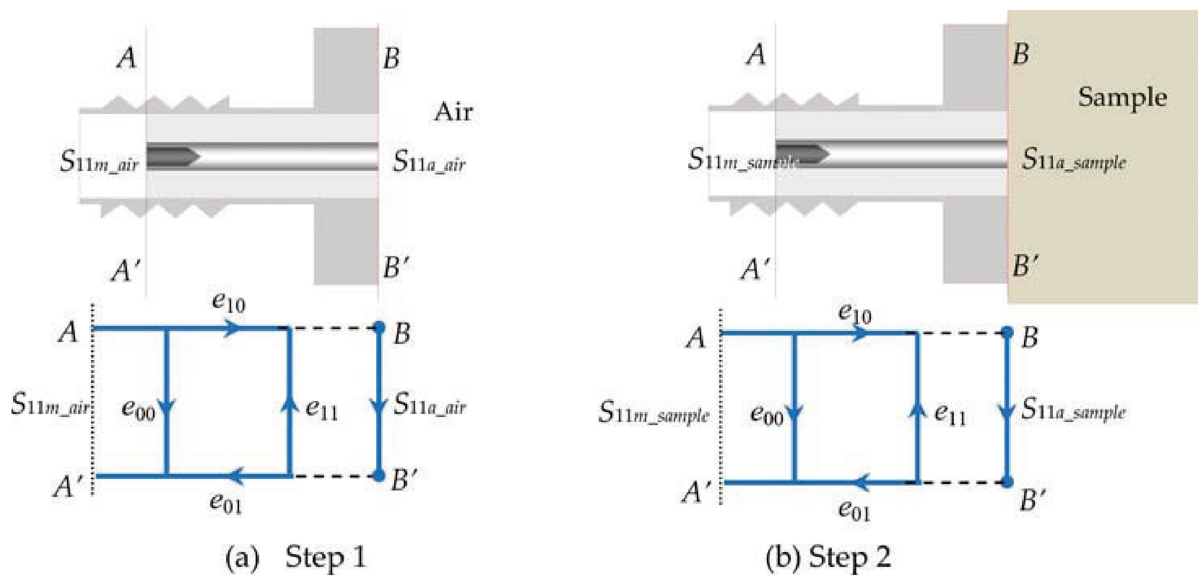

Figure 9. Error network and finite coaxial line: (a) terminated by air; (b) terminated by a sample under test.

In this subsection, a simple open standard calibration is introduced which requires the probe aperture open to the air as shown in **Figure 9a**. Firstly, the S_{11m_air} for the air is measured. Later, the probe aperture is contacted with the sample under test, and its S_{11m_sample} is measured as shown in **Figure 9b**. The relationship between the S_{11m_air} at the plane AA' and S_{11a_air} at the probe aperture BB' is expressed in a bilinear equation as:

$$S_{11a_air} = \frac{S_{11m_air} - e_{00}}{e_{11}S_{11m_air} + e_{10}e_{01} - e_{00}e_{11}} \tag{1}$$

Similarly, the relationship between measured S_{11m_sample} and S_{11a_sample} is given as:

$$S_{11a_sample} = \frac{S_{11m_sample} - e_{00}}{e_{11}S_{11m_sample} + e_{10}e_{01} - e_{00}e_{11}} \tag{2}$$

The e_{00}, e_{11} and $e_{10}e_{01}$ are the unknown scattering parameters of the error network for the coaxial line.

The e_{00} is the directivity error that causes the failure to receive the measured reflection signal completely from the sample being tested at plane BB'. The e_{11} is the source matching error due to the fact that the impedance of the aperture probe at plane BB' is not exactly the characteristic impedance (Z_o = 50 Ω). The $e_{10}e_{01}$ is the frequency tracking imperfections (or phase shift) between plane AA' and sample test plane BB'. For this calibration, the e_{00} and e_{11} terms in Eqs. (1) and (2) are assumed to be vanished ($e_{00} = e_{11} = 0$). By dividing Eq. (2) into Eq. (1), yields

$$\frac{S_{11a_sample}}{S_{11a_air}} = \frac{S_{11m_sample}}{S_{11m_air}} \tag{3}$$

Once the S_{11m_air} and S_{11m_sample} are obtained, the actual reflection coefficient, S_{11a_sample}, of the sample at the probe aperture, BB' can be found as:

$$S_{11a_sample} = \frac{S_{11a_air}}{S_{11m_air}} \times S_{11m_sample} \tag{4}$$

The standard values of the reflection coefficient, S_{11a_air} in (4), can be calculated from Eq. (5) that satisfying conditions: (DC < f < 24) GHz.

$$S_{11a_air} = \frac{1-j(\omega/Y_o)(C_o f^{-1} + C_1 + C_2 f + C_3 f^2)}{1+j(\omega/Y_o)(C_o f^{-1} + C_1 + C_2 f + C_3 f^2)} \tag{5}$$

Symbol $\omega = 2\pi f$ and $Y_o = [(2\pi)/\ln(b/a)]\sqrt{(\varepsilon_o\varepsilon_c/\mu_o\mu_r)}$ are the angular frequency (in rad/s) and characteristic admittance (in siemens), respectively. For instance, the complex values of the C_o, C_1, C_2 and C_3 in (5) for Teflon-filled coaxial probe with $2a$ = 1.3 mm, $2b$ = 4.1 mm and ε_c = 2.06 are given as [12]:

$$C_o = 5.368082994761808 \times 10^{-7} + j\, 2.320071598550666 \times 10^{-7} \quad (\mathrm{F} \times \mathrm{Hz})$$

$$C_1 = 3.002820660256831 \times 10^{-14} - j\, 2.988971515445163 \times 10^{-16} \quad (\mathrm{F})$$

$$C_2 = 1.112989441958266 \times 10^{-25} + j\, 7.730261500907114 \times 10^{-26} \quad (\mathrm{F/Hz})$$

$$C_3 = 3.140652268416283 \times 10^{-36} - j\, 6.786433840933426 \times 10^{-36} \quad (\mathrm{F/Hz^2})$$

It should be noted that this simple calibration technique will not eliminate the standing wave effects in the coaxial line.

3.1.2. Open-short-load (OSL) standard calibrations

In this subsection, the three-standard calibration is reviewed in which open, short and load standards are used in the de-embedding process [13]. Let S_{11a_a}, S_{11a_s} and S_{11a_w} represent the known reflection coefficients for the open, short and load (water) standards which are terminated at the aperture plane BB', while S_{11m_a}, S_{11m_s} and S_{11m_w} are the measured reflection coefficients for open, short and load standards at plane AA'. The S_{11m_a} is measured by leaving

the open end of the probe in the air as shown in **Figure 10a**. Later, the measurement is repeated to obtain the S_{11m_s} by terminating the probe aperture with a metal plate as shown in **Figure 10b**. Finally, the S_{11m_w} is obtained by immersing the probe in water as shown in **Figure 10c**.

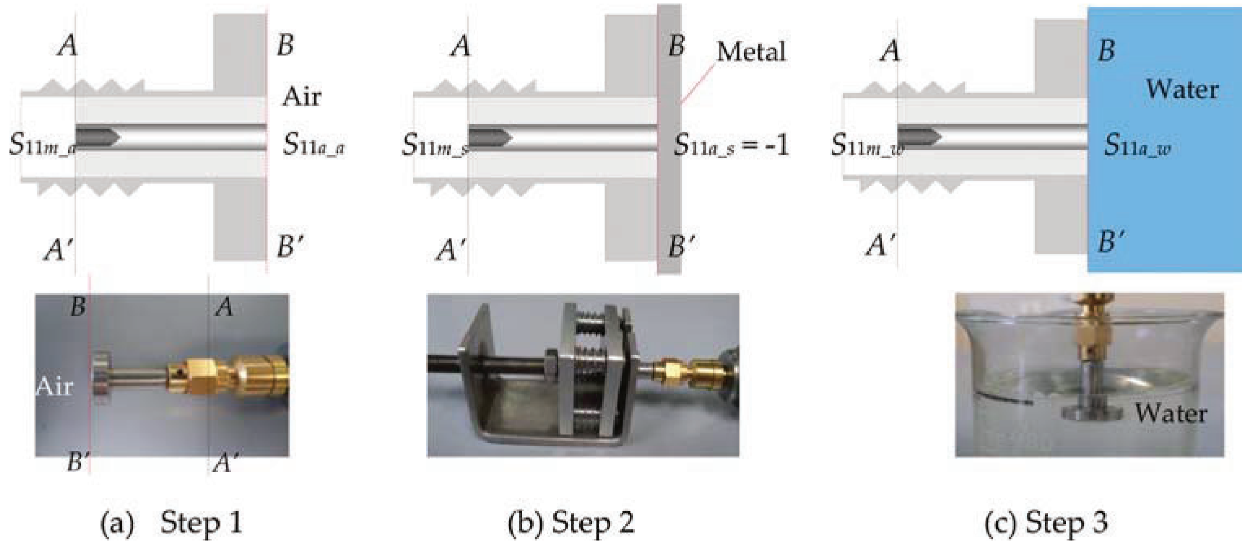

Figure 10. Finite coaxial line: (a) terminated by free space; (b) shorted by a metal plate; (c) immersed in water.

Once the complex values of S_{11a_air}, S_{11a_short}, S_{11a_water}, S_{11m_a}, S_{11m_s} and S_{11m_w} are known, the three unknown complex coefficients (e_{00}, e_{11}, and $e_{10}e_{01}$) values in Eq. (2) can be found as:

$$e_{00} = \frac{S_{11a_s}S_{11a_w}S_{11m_a}\Delta_{w_s} + S_{11a_o}S_{11a_s}S_{11m_w}\Delta_{s_a} + S_{11a_a}S_{11a_w}S_{11m_s}\Delta_{a_w}}{S_{11a_w}S_{11a_s}\Delta_{w_s} + S_{11a_a}S_{11a_s}\Delta_{s_a} + S_{11a_w}S_{11a_a}\Delta_{a_w}} \tag{6a}$$

$$e_{11} = \frac{-(S_{11a_a}\Delta_{w_s} + S_{11a_w}\Delta_{s_a} + S_{11a_s}\Delta_{a_w})}{S_{11a_w}S_{11a_s}\Delta_{w_s} + S_{11a_a}S_{11a_s}\Delta_{s_a} + S_{11a_w}S_{11a_a}\Delta_{a_w}} \tag{6b}$$

$$e_{10}e_{01} = (e_{00} \times e_{11}) + \frac{S_{11a_a}S_{11m_a}\Delta_{w_s} + S_{11a_w}S_{11m_w}\Delta_{s_a} + S_{11a_s}S_{11m_s}\Delta_{a_w}}{S_{11a_w}S_{11a_s}\Delta_{w_s} + S_{11a_a}S_{11a_s}\Delta_{s_a} + S_{11a_w}S_{11a_a}\Delta_{a_w}} \tag{6c}$$

where

$\Delta_{a_w} = S_{11m_a} - S_{11m_w}$, $\Delta_{s_a} = S_{11m_s} - S_{11m_a}$, and $\Delta_{w_s} = S_{11m_w} - S_{11m_s}$

3.1.3. Short-offset-offset short (SOO) standard calibrations

The open-short-load (OSL) technique is rarely used in the one-port rectangular waveguide calibration due to unavailable commercial open kit for the rectangular waveguide. In this subsection, the short-offset-offset short (SOO) calibration [14, 15] is introduced for waveguide calibration by using waveguide adjustable sliding shorts as shown in **Figure 11**. The calibration procedures are shown in **Figure 12**.

In this calibration method, the measured reflection coefficients for one shorted aperture and two different lengths, l of offset short are required. Let S_{11m_1}, S_{11m_2} and S_{11m_3} represent the known measured reflection coefficients at plane AA' for the shorted aperture and the two offset shorts at location l_1 and l_2 from the waveguide aperture, respectively. Before calibration, the selection of the appropriate offset short length, l_1 and l_2 will be an issue. The lengths of the offset shorts can be determined by conditions:

1. The three phase shift between the S_{11m_1}, S_{11m_2} and S_{11m_3} must not be equal:

$$\angle(S_{11m_2})-\angle(S_{11m_1})\neq\angle(S_{11m_3})-\angle(S_{11m_1})\neq\angle(S_{11m_3})-\angle(S_{11m_2})$$

2. The resolution degree between any three phase shift must be significant large (>100°) as shown in **Figure 13**. In this work, the distance l_1 and l_2 for the offset shorts from the X-band waveguide aperture are equal to 0.007 m and 0.013 m, respectively.

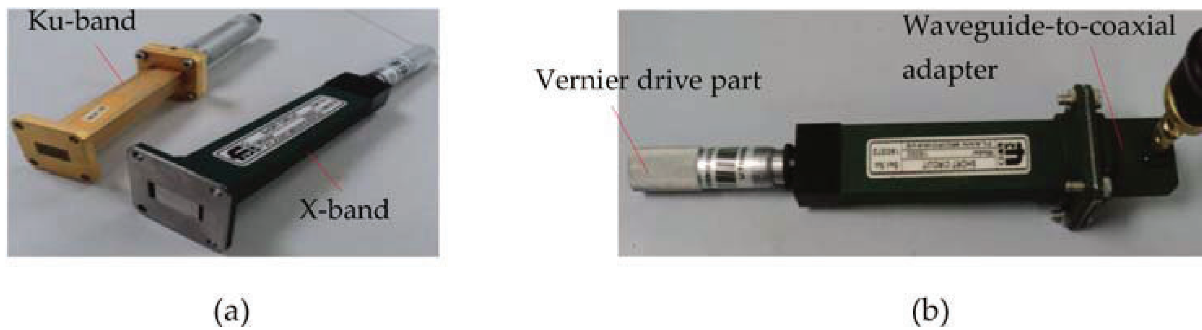

Figure 11. (a) Ku-band and X-band waveguide adjustable sliding shorter. (b) Connection between sliding short with waveguide-to-coaxial adapter.

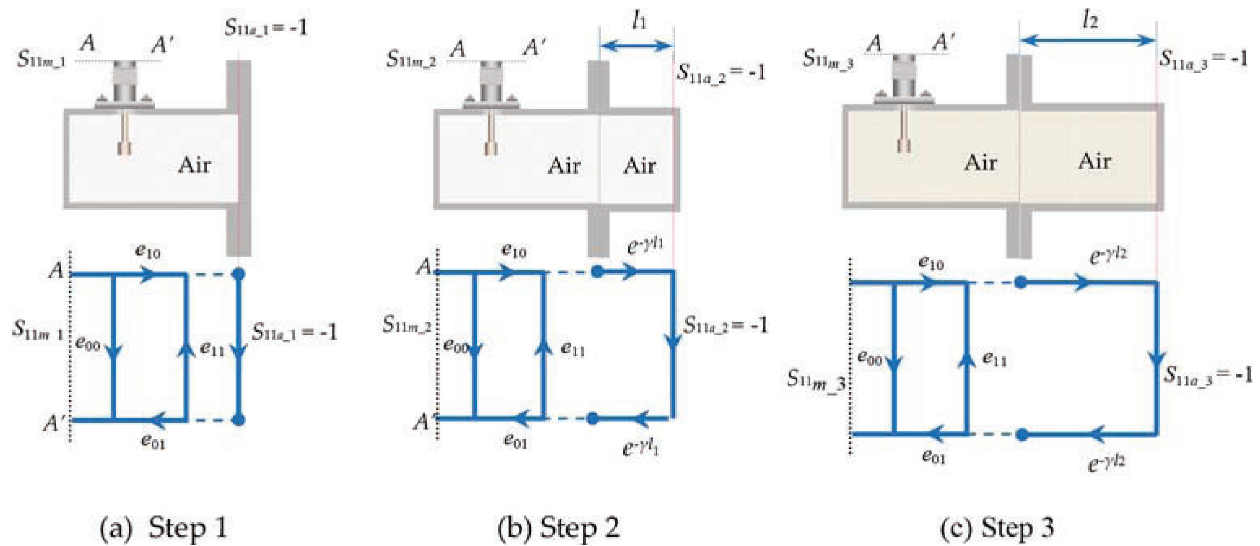

Figure 12. Calibration procedures of the aperture rectangular waveguide using an adjustable shorter. (a) Step 1; (b) Step 2; (c) Step 3

http://dx.doi.org/10.5772/66230

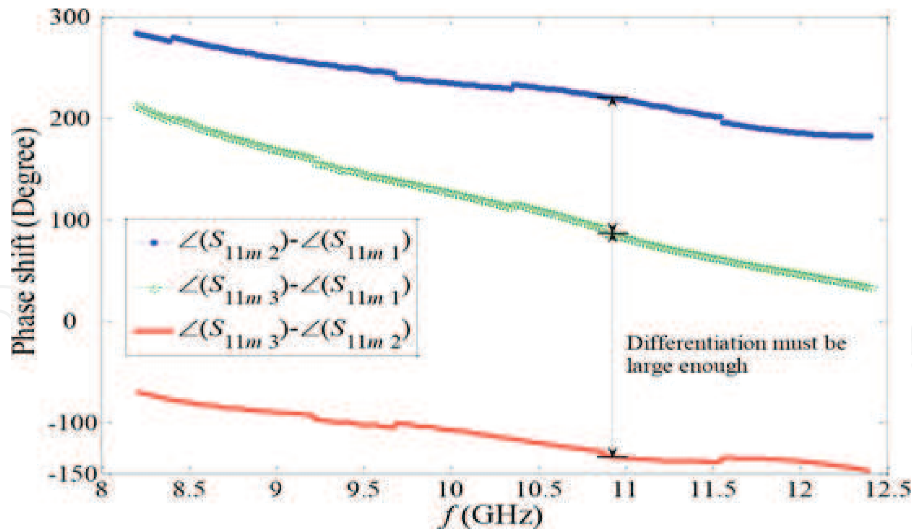

Figure 13. The three phase shift of the measured reflection coefficients for the shorted aperture and two offset shorts with l_1 = 0.7 cm and l_2 = 1.3 cm, respectively.

Once the S_{11m_1}, S_{11m_2}, S_{11m_3}, l_1 and l_2 are obtained, the three unknown complex coefficients (e_{00}, e_{11}, and $e_{10}e_{01}$) values in Eq. (2) can be found as:

$$e_{00} = \frac{S_{11m_1}S_{11m_2}(e^{-2\gamma l_1}-1)-S_{11m_2}S_{11m_3}\left(e^{2\gamma(l_2-l_1)}-1\right)-S_{11m_1}S_{11m_3}\left(e^{-2\gamma l_1}-e^{2\gamma(l_2-l_1)}\right)}{(e^{-2\gamma l_1}-1)(S_{11m_2}-S_{11m_3})-\left(e^{2\gamma(l_2-l_1)}-1\right)(S_{11m_2}-S_{11m_1})} \tag{7a}$$

$$e_{11} = \frac{e^{2\gamma l_1}(S_{11m_2}-e_{00}) + e_{00}-S_{11m_1}}{S_{11m_1}-S_{11m_2}} \tag{7b}$$

$$e_{10}e_{01} = (e_{00}-S_{11m_1})(1+e_{11}) \tag{7c}$$

The complex reflection coefficient, S_{11a_sample}, at the waveguide aperture which is open to the air was measured. Then, the measured S_{11a_sample} was converted to normalized admittance, Y/Y_o parameter by a formula: $Y/Y_o = (1 - S_{11a_sample})/(1 + S_{11a_sample})$. The SOO calibration techniques were validated by comparing normalized admittance, Y/Y_o with the literature data [15–22] as shown in **Figure 14**. The real part, Re(Y/Y_o), and the imaginary part, Im(Y/Y_o), of admittance results were found to be in good agreement with literature data over the operational range of frequencies.

3.2. Two-port calibrations [through-reflect-line (TRL)]

The through-short-line (TRL) calibration model [23] is used for two-port rectangular waveguide measurement. The TRL technique requires three standards, which are *through*, *short* and *line* measurements at the CC' and DD' planes so-called reference planes (at the front surface of the sample under test) as shown in **Figure 15**.

The error coefficients (e_{00}, e_{11}, $e_{10}e_{01}$, e_{33}, e_{22}, e_{32}, and e_{23}) in **Figure 15** can be obtained by solving the matrix equation of Eq. (8).

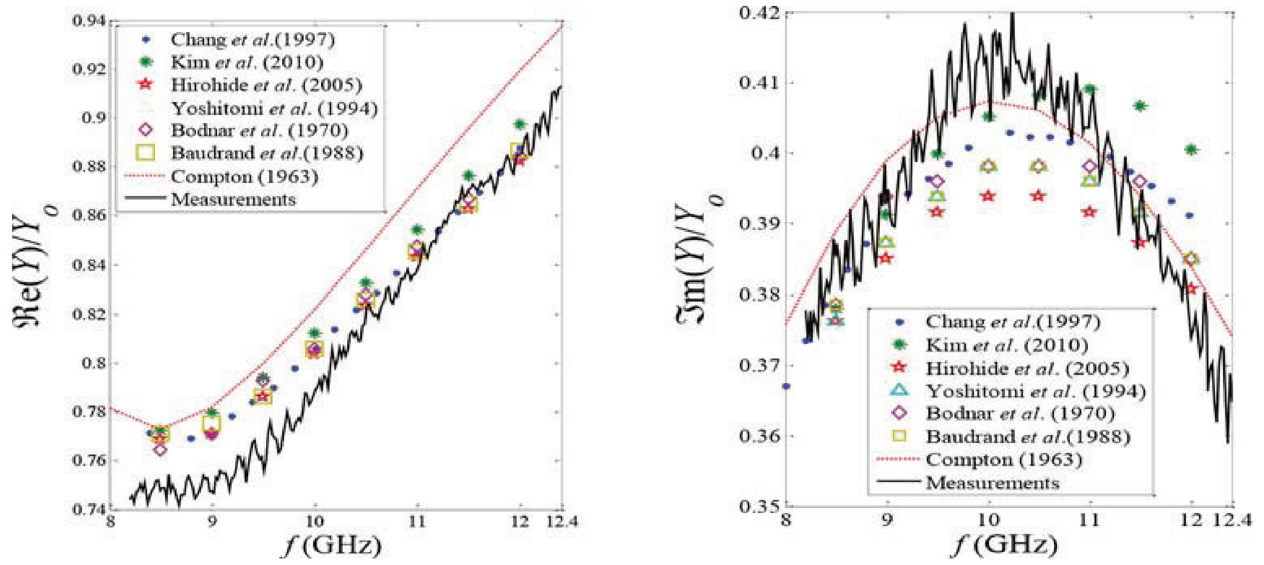

Figure 14. Comparison of real part, Re(Y/Y_o), and imaginary part, Im(Y/Y_o), of the normalized admittance for air.

$$\begin{bmatrix} 1 & 0 & 0 & 0 & S_{12m_Thru} & 0 & 0 & 0 & 0 & 0 & 0 & 0 \\ 0 & S_{11m_Thru} & -1 & 0 & 0 & 0 & -S_{12m_Thru} & 0 & 0 & 0 & 0 & 0 \\ 0 & 0 & 0 & 0 & S_{22m_Thru} & -1 & 0 & 0 & 0 & 0 & 0 & 0 \\ 0 & S_{21m_Thru} & 0 & 1 & 0 & 0 & -S_{22m_Thru} & 0 & 0 & 0 & 0 & 0 \\ 1 & -S_{11m_Short} & 1 & 0 & 0 & 0 & 0 & 0 & 0 & 0 & 0 & 0 \\ 0 & 0 & 0 & 0 & -S_{12m_Short} & 0 & -S_{12m_Short} & 0 & 0 & 0 & 0 & 0 \\ 0 & -S_{21m_Short} & 0 & 0 & 0 & 0 & 0 & 0 & 0 & 0 & 0 & 0 \\ 0 & 0 & 0 & 1 & -S_{22m_Short} & 1 & -S_{22m_Short} & 0 & 0 & 0 & 0 & 0 \\ 1 & 0 & 0 & 0 & e^{-j\beta l}S_{12m_Line} & 0 & 0 & 0 & 0 & 0 & 0 & 0 \\ 0 & e^{j\beta l}S_{11m_Line} & e^{j\beta l} & 0 & 0 & 0 & -S_{12m_Line} & 0 & 0 & 0 & 0 & 0 \\ 0 & 0 & 0 & 0 & e^{-j\beta l}S_{22m_Line} & -e^{-j\beta l} & 0 & 0 & 0 & 0 & 0 & 0 \\ 0 & e^{j\beta l}S_{21m_Line} & 0 & 1 & 0 & 0 & -S_{22m_Line} & 0 & 0 & 0 & 0 & 0 \end{bmatrix} \begin{bmatrix} e_{00} \\ e_{11} \\ \Delta_x \\ ke_{33} \\ ke_{22} \\ k\Delta_y \\ k \\ 0 \\ 0 \\ 0 \\ 0 \\ 0 \end{bmatrix} = \begin{bmatrix} S_{11m_Thru} \\ 0 \\ S_{21m_Thru} \\ 0 \\ S_{11m_Short} \\ 0 \\ S_{21m_Short} \\ 0 \\ S_{11m_Line} \\ 0 \\ S_{21m_Line} \\ 0 \end{bmatrix} \tag{8}$$

where $k = e_{10}/e_{23}$, $\Delta_x = e_{00}e_{11} - e_{10}e_{01}$ and $\Delta_y = e_{22}e_{33} - e_{32}e_{23}$. Once the S_{11m_sample}, S_{21m_sample}, S_{12m_sample} and S_{22m_sample} at plane AA' and BB' for the sample under test are measured, the calibrated reflection coefficient, S_{11a_sample} at plane CC' and transmission coefficient, S_{21a_sample} at plane DD' can be calculated as:

$$S_{11a_sample} = \frac{\left\{ \begin{array}{l} \left(\frac{S_{11m_sample} - e_{00}}{e_{10}e_{01}}\right)\left[1 + \left(\frac{S_{22m_sample} - e_{33}}{e_{23}e_{32}}\right)e_{22}\right] \\ -e_{22}\left(\frac{S_{21m_sample} - S_{21m_Thru}}{e_{10}e_{32}}\right)\left(\frac{S_{12m_sample} - S_{12m_Thru}}{e_{23}e_{01}}\right) \end{array} \right\}}{D} \tag{9a}$$

$$S_{21a_sample} \cong \frac{\left(\frac{S_{21m_sample} - S_{21m_Thru}}{e_{10}e_{32}}\right)}{D} \tag{9b}$$

The denominator, D in (9a) and (9b) is given as:

IntechOpen

http://dx.doi.org/10.5772/66230

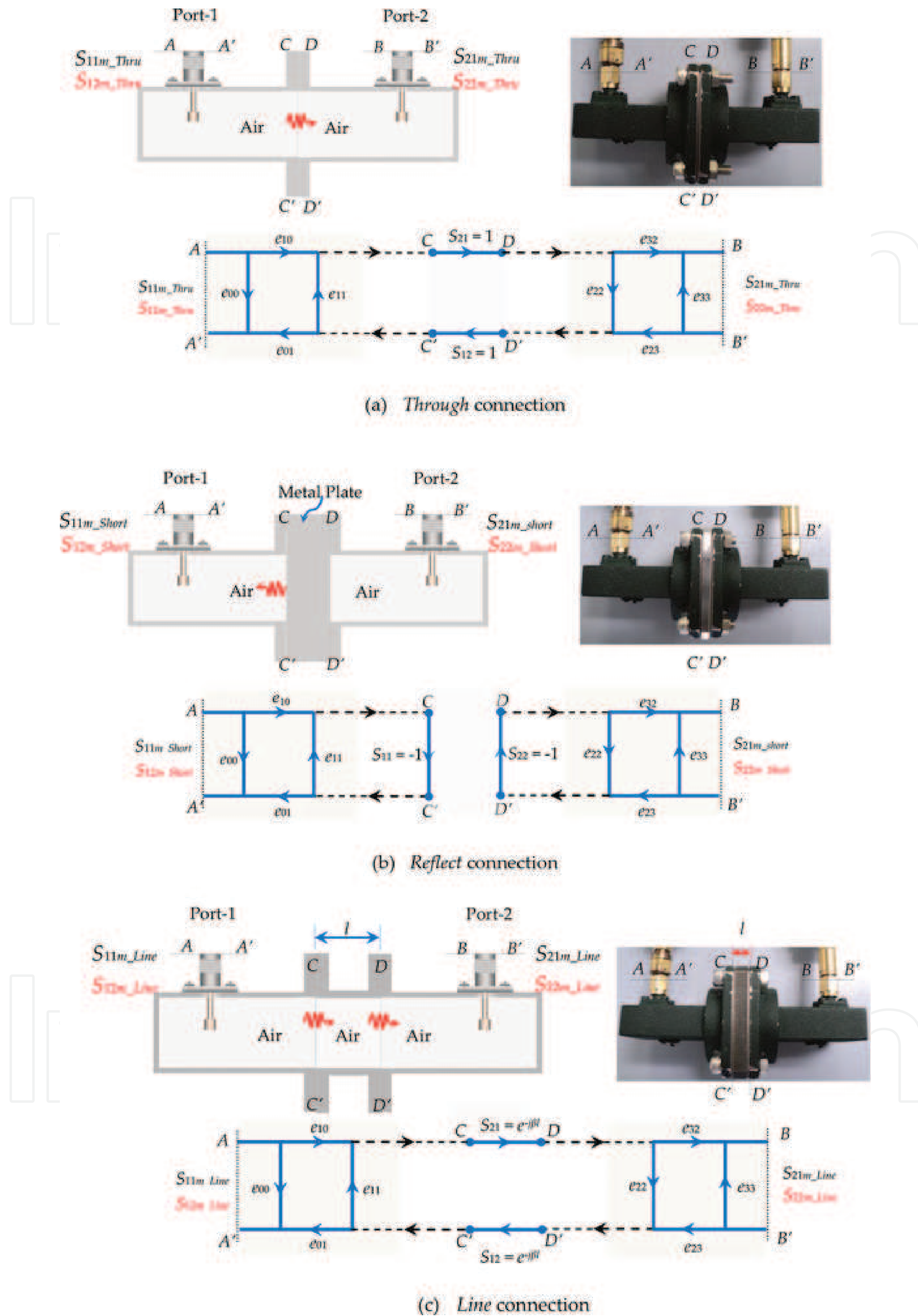

Figure 15. through-short-line (TRL) calibration procedures and its network errors. *(a) Through* connection; *(b) Reflect* connection; *(c) Line* connection.

$$D = \left\{ \begin{array}{l} \left[1 + \left(\frac{S_{11m_sample} - e_{00}}{e_{10}e_{01}}\right)e_{11}\right]\left[1 + \left(\frac{S_{22m_sample} - e_{33}}{e_{23}e_{32}}\right)e_{22}\right] \\ -\left(\frac{S_{21m_sample} - S_{21m_Thru}}{e_{10}e_{32}}\right)\left(\frac{S_{12m_sample} - S_{12m_Thru}}{e_{23}e_{01}}\right)e_{22}e_{11} \end{array} \right\}$$

4. Material parameters extraction

4.1. Reflection measurements (one-port measurements)

There are two methods of determining sample parameters (ε_r, μ_r or σ), which are the direct method and the inverse method. The direct method involves the explicit model to predict the sample under test based on the measured reflection coefficient, S_{11a_sample}, while the inverse method is implemented rigorous integral admittance model to estimate the sample parameters (ε_r, μ_r or σ) using optimization procedures. For coaxial probe measurement cases, the explicit relationship between ε_r and S_{11a_sample} [8] is tabulated in **Table 1**. For rectangular waveguide cases, the measured S_{11a_sample} is transferred to normalized admittance, $\tilde{Y}_{a_sample}$ through equation: $\tilde{Y}_{a_sample} = (1 - S_{11a_sample})/(1 + S_{11a_sample})$. The predicted value of ε_r is obtained by minimizing the difference between the measured normalized admittance, $\tilde{Y}_{a_sample}$ and the quasi-static integral model, $\tilde{Y}$ (in **Table 2**) [9, 17] by referring to particular objective function. The procedures of direct method are more straightforward than the inverse method. The detail descriptions of the parameters (Y_o, C and γ_o) and the coefficients (a_1, a_2 and a_3) in Eqs. (10)–(13) can be found in [8, 9, 17].

4.2. Reflection/transmission measurements (two-port measurements)

Conventionally, the complex $\varepsilon_r = \varepsilon_r' - j\varepsilon_r''$ and the $\mu_r = \mu_r' - j\mu_r''$ of the sample filled in the coaxial or rectangular waveguide are obtained by converting the calibrated reflection coefficient, $S_{11\boldsymbol{a_sample}}$ and the transmission coefficient, $S_{21\boldsymbol{a_sample}}$ by using Nicholson-Ross-Weir (NRW) routines [10, 11]. In this section, another alternative method, namely transmission phase shift (TPS) method [24], is reviewed. The TPS method is a calibration-independent and material position-invariant technique, which can reduce the complexity of the de-embedding procedures. The important formulations of the NRW and the TPS methods are tabulated in **Table 3**.

Sample cases	Open-ended coaxial probe
Semi-infinite space sample (**Figure 5a**)	$\varepsilon_r = \left(\frac{Y_o}{j\omega C}\right)\left(\frac{1 - S_{11a_sample}}{1 + S_{11a_sample}}\right)$ (10)
Thin sample backed by metal plate (**Figure 5b**)	$\varepsilon_r = \left(\frac{Y_o}{j\omega C}\right)\left(\frac{1 - S_{11a_sample}}{1 + S_{11a_sample}}\right)(a_1 + a_2 e^{-d/M} + a_3 e^{-2d/M})$ (11)

Table 1. Explicit formulations for open-ended coaxial probe.

Sample cases	Open-ended rectangular waveguide
Semi-infinite space sample (**Figure 5c**)	$$\tilde{Y}=\frac{j8b}{a\gamma_o}\int_0^a\int_0^b\left\{(a-x)\left\{D_1(b-y)\cos\frac{\pi y}{b}+D_2\sin\frac{\pi y}{b}\right\}\times\frac{\exp\left(-jk_1\sqrt{x^2+y^2}\right)}{\sqrt{x^2+y^2}}\right\}dxdy \quad (12)$$ where $D_1=\frac{1}{b^2}\left(\frac{k_1^2}{4\pi}-\frac{\pi}{4b^2}\right)$, $D_2=\frac{1}{\pi b}\left(\frac{k_1^2}{4\pi}+\frac{\pi}{4b^2}\right)$, and $k_1=\frac{2\pi f}{c}\sqrt{\varepsilon_r}$
Thin sample backed by metal plate (**Figure 5d**)	$$\tilde{Y}=\frac{j8b}{a\gamma_o}\int_0^a\int_0^b\chi\frac{\exp\left(-jk_1\sqrt{x^2+y^2}\right)}{\sqrt{x^2+y^2}}dxdy+\frac{j16b}{a\gamma_o}\sum_{n=1}^{\infty}\int_0^a\int_0^b\chi\frac{\exp\left(-jk_1\sqrt{x^2+y^2+4n^2d^2}\right)}{\sqrt{x^2+y^2+4n^2d^2}}dxdy \quad (13)$$ where $\chi=(a-x)\left\{D_1(b-y)\cos\frac{\pi y}{b}+D_2\sin\frac{\pi y}{b}\right\}$

Table 2. Integral admittance formulations for open-ended rectangular waveguide.

	Waveguide factors	Explicit equations
NRW method [10–11]	Coaxial: $\zeta=1$ Waveguide: $\zeta=\sqrt{k_o^2-\left(\frac{\pi}{b}\right)^2}$	$$\varepsilon_r=j\zeta\left(\frac{1-\Gamma}{1+\Gamma}\right)\left(\frac{c}{2\pi fd}\right)\ln\left(\frac{1}{T}\right) \quad (14a)$$ $$\mu_r=j\frac{1}{\zeta}\left(\frac{1+\Gamma}{1-\Gamma}\right)\left\{\frac{c}{2\pi fd}\ln\left(\frac{1}{T}\right)\right\} \quad (14b)$$
TPS method [24]	Coaxial: $\xi=0$ and $\gamma_o=k_o$ Waveguide: $\xi=\left(\frac{\pi}{b}\right)^2\gamma_o=\sqrt{k_o^2-\left(\frac{\pi}{b}\right)^2}$	$$\varepsilon'_r=\frac{1}{k_o^2}\left\{\left(\gamma_o+\frac{\phi_{21_air}-\phi_{21_sample}}{d}\right)^2+\xi-\alpha^2\right\} \quad (15a)$$ $$\varepsilon''_r=\frac{2\alpha}{k_o^2}\left(\gamma_o+\frac{\phi_{21_air}-\phi_{21_sample}}{d}\right) \quad (15b)$$

Table 3. Explicit formulations for reflection/transmission measurements.

where $k_o = 2\pi f/c$ is the propagation constant of free space (c = 2.99792458 ms^{-1}); b (in meter) are the width of the aperture of the waveguide, respectively; d(in meter) is the thickness of the sample. The expressions for parameters Γ and T in Eqs. (14a, b) can be found in [10, 24]. The ϕ_{21_air} and ϕ_{21_sample} in Eqs. (15a, b) are the measured phase shift of the transmission coefficient

in the air (without sample) and the sample, respectively. On the other hand, symbol α (in nepers/meter) is the dielectric attenuation constant for the sample.

You et al. [24] have been mentioned that the uncertainty of the permittivity measurement is high for the low-loss thin sample by using TPS method due to the decreasing of the sensitivity for the transmitted wave through the thin sample, especially for transmitted waves that have longer wavelengths. However, the literature [24] did not discuss how the thickness of the thin sample may affect the uncertainty of measurement using TPS technique in quantitative. From this reasons, the TPS method is reexamined in this section. Various thicknesses of acrylic, FR4 and RT/duroid 5880 substrate samples were placed in the X-band rectangular waveguide and measured for validation. **Figure 16a–c** shows the predicted dielectric constant, ε_r' of the samples using Eq. (15a) at 8.494, 10.006 and 11.497 GHz, respectively. Clearly, the TPS method is capable of providing a stable and accurate measurement for operating frequency in X-band range when the thicknesses of the samples have exceeded 2 cm [25].

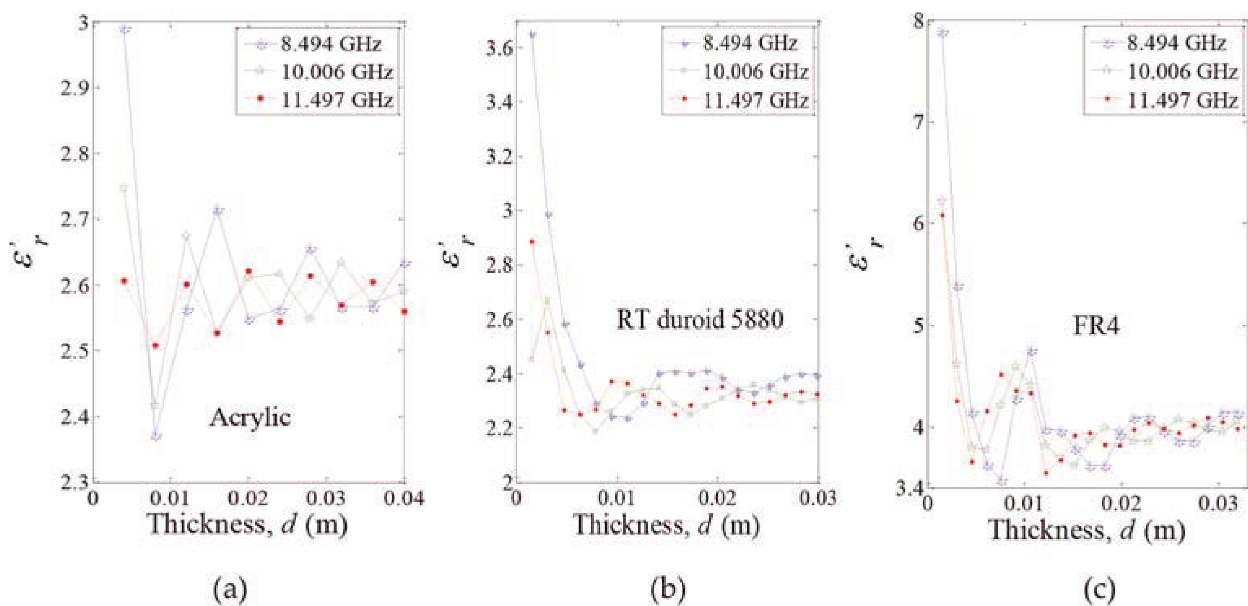

Figure 16. Variations in relative dielectric constant, ε_r with the thickness layer of (a) acrylic, (b) RT/duroid 5880 substrate and (c) FR4, respectively.

5. Conclusion

The brief background of the microwave waveguide techniques for materials characterization is reviewed and summarized. Not only that the measurement methods play an important role, the calibration process is crucial as well. However, most of the literatures have ignored the description of calibration. Measurement without calibration certainly cannot predict the properties of materials accurately. Thus, in this chapter, some of the waveguide calibrations are described in detail.

Author details

Kok Yeow You

Address all correspondence to: kyyou@fke.utm.my

Department of Communication Engineering, Faculty of Electrical Engineering, Universiti Teknologi Malaysia, Johor, Malaysia

IntechOpen

References

[1] Hakki B W, Coleman P D: A dielectric resonator method of measuring inductive capacities in the millimeter range. IRE Transactions on Microwave Theory and Techniques. 1960; **8(7)**: 402–410.

[2] Courtney W E: Analysis and evaluation of a method of measuring the complex permittivity and permeability of microwave insulators. IEEE Transactions on Microwave Theory and Techniques. 1970; **18(8)**: 476–485.

[3] Tosaka T, Fujii K, Fukunaga K, Kasamatsu A: Development of complex relative permittivity measurement system based on free-space in 220–330 GHz range. IEEE Transaction on Terahertz Science and Technology. 2015; **5(1)**: 102–109.

[4] Abbas Z, Pollard R D, Kelsall R W: Complex permittivity measurements at Ka-Band using rectangular dielectric waveguide. IEEE Transactions on Instrumentation and Measurement. 2001; **50(5)**: 1334–1342.

[5] Kemptner E, Thurner S: Free space material characterization for microwave frequencies. 6th European Conference on Antennas and Propagation (EUCAP). 2011: 3513–3515.

[6] You K Y, Mun H K, You L L, Jamaliah S, Abbas Z: Small and slim coaxial probe for single rice grain moisture sensing. Sensors. 2013;**13(3)**: 3652–3663.

[7] You K Y, Jamaliah S, Abbas Z: Effects of length and diameter of open-ended coaxial sensor on its reflection coefficient. RadioEngineering. 2012; **21(1)**: 496–503.

[8] You K Y, Then Y L: Simple calibration and dielectric measurement technique for thin material using coaxial probe. IEEE Sensors Journal. 2015; **15(10)**: 5393–5397.

[9] You K Y, Abbas Z, Malek M F A, Cheng E M: Non-destructive dielectric measurements and calibration for thin materials using waveguide-coaxial adaptors. Measurement Science Review. 2014; **14(1)**: 16–24.

[10] Nicolson A M, Ross G F: Measurement of the intrinsic properties of materials by time-domain techniques. IEEE Transactions on Instrumentation and Measurement. 1970; **19(4)**: 377–382.

IntechOpen

[11] Weir W B: Automatic measurement of complex dielectric constant and permeability at microwave frequencies. Proceedings of the IEEE. 1974; **62(1)**: 33–36.

[12] You K Y. RF Coaxial Slot Radiators: Modeling, Measurements, and Applications. USA: Artech House; 2015. ISBN: 978-1-60807-822-6.

[13] Kraszewski A, Stuchly M A, Stuchly S S: ANA calibration method for measurements of dielectric properties. IEEE Transactions on Instrumentation and Measurement. 1983; **32 (2)**: 385–386.

[14] Da Silva E F, McPhun M K: Calibration techniques for one-port measurement. Microwave Journal. 1978; **21(6)**: 97–100.

[15] Chang C W, Chen K M, Qian J: Nondestructive determination of electromagnetic parameters of dielectric materials at X-band frequencies using a waveguide probe system. IEEE Transactions on Instrumentation and Measurement. 1997; **46(5)**: 1084–1092.

[16] Kim J H, Enkhbayar B, Bang J H, Ahn B C:New formulas for the reflection coefficient of an open-ended rectangular waveguide radiating into air including the effect of wall thickness or flange. Progress in Electromagnetics Research M. 2010; **12**: 143–153.

[17] Compton R T Jr. The Aperture Admittance of a Rectangular Waveguide Radiating into a Lossy Half-Space. Technical Report, 1691-1, Columbus, Ohio: Ohio State University; 1963.

[18] Ganchev S I, Bakhtiari S, Zoughi R: A novel numerical technique for dielectric measurement of generally lossy dielectrics. IEEE Transactions on Instrumentation and Measurement. 1992; **41(3)**: 361–365.

[19] Yoshitomi K, Sharobim H R: Radiation from a rectangular waveguide with a lossy flange. IEEE Transactions on Antennas and Propagation.1994; **42(10)**: 1398–1403.

[20] Hirohide, Serizawa, Hongo K: Radiation for a flanged rectangular waveguide. IEEE Transactions on Antennas and Propagation.2005; **53(12)**: 3953–3962.

[21] Bodnar D G, Paris D T: New variational principle in electromagnetic. IEEE Transactions on Antennas and Propagation.1970; **18(2)**: 216–223.

[22] Baudrand H, Tao J, Atechian J: Study of radiation properties of open-ended rectangular waveguides. IEEE Transactions on Antennas and Propagation. 1988; **36(8)**: 1071–1077.

[23] Engen G F, Hoer C A: Thru-reflect-line: an improved technique for calibrating the dual six-port automatic network analyzer. IEEE Transactions on Microwave Theory and Techniques. 1979; **27(12)**: 987–993.

[24] You K Y, Lee Y S, Zahid L, Malek M F A, Lee K Y, Cheng E M: Dielectric measurements for low-loss materials using transmission phase-shift method. JurnalTeknologi. 2015; **77 (10)**: 69–77.

[25] You K Y: Effects of sample thickness for dielectric measurements using transmission phase-shift method. International Journal of Advances in Microwave Technology. 2016; **1(3)**: 64–67.